Three-dimensional model for light-induced chaotic rotations in liquid crystals under spin and orbital angular momentum transfer processes

Etienne Brasselet
Centre de Physique Moléculaire Optique et Hertzienne, Université Bordeaux 1, CNRS, 351 Cours de la Libération, 33405 Talence Cedex, France

Bruno Piccirillo* and Enrico Santamato*
Dipartimento di Scienze Fisiche, Università di Napoli "Federico II," via Cintia, 80126 Napoli, Italy
(Received 9 April 2008; revised manuscript received 22 August 2008; published 3 September 2008)

Liquid crystals interacting with light represent a unique class of soft-matter systems that exhibit various generic nonlinear behaviors, including chaotic rotational dynamics. Despite several experimental observations, complex nematic liquid crystal director rotations in presence of spin and orbital angular momentum transfer processes were left unexplained. We present a self-consistent three-dimensional model able to describe the previous experimental observations, accounting for the dependence on the incident beam intensity, polarization, finite size and shape. More generally, our model is able to describe quantitatively the dynamics of, and beyond, the optical Fréedericksz transition under realistic experimental conditions almost three decades after its experimental discovery.

DOI: 10.1103/PhysRevE.78.031703 PACS number(s): 42.70.Df, 05.45.−a, 42.65.Sf

I. INTRODUCTION

Dynamical systems that are described by a set of coupled first-order autonomous differential equations are usually characterized in terms of rotational motions, which is a generic feature of many processes in physics, chemistry, or biology. This is especially the case when such nonlinear systems exhibit chaotic dynamics. Then, the system trajectory can be considered as going through an infinite number of rotationlike motions characterized by a suitable definition of the phase [1], which is of special interest in the framework of phase synchronization [2,3]. Due to the modeling difficulties and/or achievable computational handling of real dynamical systems exhibiting chaotic rotations, their description is usually reduced to standard nonlinear models, such as the Lorentz [4] or Rössler [5] systems. Exact modeling of real systems exhibiting chaotic rotations is much less widespread.

Quite recently, chaotic rotations generated by a light field in nematic liquid crystals (NLCs) have been reported [6,7]. In these experiments, the light was circularly polarized and sent at normal incidence onto a homeotropically aligned nematic film. In Ref. [6] an elliptically shaped light beam was used, while in Ref. [7] the incident beam shape was cylindrically symmetric. In both cases the observations were left unexplained despite some attempt to describe the NLC continuum medium as a discrete set of coupled nonlinear rotators driven by light, which led to a generic Kuramoto model [7,8]. The major difficulty in modeling this kind of experiment is that the dynamics of the NLC director is strongly affected by the finite size and shape of the incoming light beam so that the plane-wave approach, where all the fields depend on one coordinate only, is inapplicable. All the three space coordinates and time must be retained. A previous attempt to model complex rotational dynamics accounting for the finite size of the light beam, but neglecting higher order reorientational modes and nonadiabatic propagation of light in the distorted liquid crystal, failed to retrieve experimental observations [9] and to give the expected sequence of bifurcations in the plane-wave limit [10]. Therefore a suitable model is still lacking.

In this paper, we present the derivation of a set of coupled ordinary differential equations (ODEs) for the motion of the local averaged molecular orientation defined by a unit vector $\boldsymbol{n}$, called director, from the fundamental equations for LCs and electromagnetic waves. The dependence of the liquid crystal dynamics on the incident beam intensity, polarization, finite size and shape are obtained, which naturally accounts for spin angular momentum (SAM) and orbital angular momentum (OAM) transfer processes between light and matter. This is another interesting yet intriguing feature of this class of experiments where both the photon SAM and OAM come into play and couple with the NLC anisotropic fluid. The model capabilities are illustrated in the case where SAM and OAM transfer processes are simultaneously present and a successful description of the complex sequence of director rotations observed in Ref. [6] is obtained. More generally, our model is able to describe quantitatively the dynamics of, and beyond, the optical Fréedericksz transition (OFT) under realistic experimental conditions almost three decades after its experimental discovery.

From a general point of view, the angular momentum balance in NLCs can be written in the form [11] $\rho(\boldsymbol{r}\times\dot{\boldsymbol{v}})=\mathrm{div}\,\hat{L}+\boldsymbol{w}$ and $\mathcal{I}(\boldsymbol{n}\times\dot{\boldsymbol{n}})=\mathrm{div}\,\hat{S}-\boldsymbol{w}$ where an upper dot stands for partial time derivative, ρ, $\mathcal{I}$, and $\boldsymbol{v}$ are, respectively, the density, inertial momentum, and velocity field of the fluid, $\hat{L}$ and $\hat{S}$ are the orbital and spin total (matter+light) angular momentum flux tensors and, finally, $\boldsymbol{w}$ is the internal torque density due to the anisotropy of the elastic constants of the material. Note that $\hat{L}$ and $\hat{S}$ can be uniquely split into a mat-

*Also at Consorzio Nazionale Interuniversitario per la Struttura della Materia (CNISM), Sezione di Napoli, Italy.

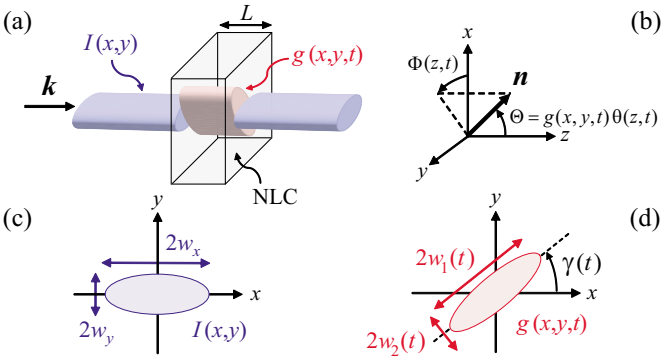

FIG. 1. (Color online) (a) Homeotropically aligned NLC film with thickness L illuminated at normal incidence by an elliptically shaped Gaussian beam with intensity distribution $I(x,y)$. (b) Representation of the director using spherical angles Θ and Φ. (c) Waists for the light beam intensity profile. (d) Waists for the director reorientation profile.

ter and an optical part, and the latter is proven to coincide with the photon orbital and spin angular momentum flux carried by the incident beam. While the matter part of $\hat{L}$ depends on the transverse gradients of $\boldsymbol{n}$ and requires a transverse inhomogeneous elastic distortion of the NLCs, its optical part depends on the gradients of the optical field and requires a light beam having a finite cross section. The internal torque $\boldsymbol{w}$ is given by the axial vector associated to the skew-symmetric part of the NLC stress tensor and represents the torque per unit volume exerted by the internal degree of freedom $\boldsymbol{n}$ on the flow [12]. It originates from the lack of invariance of the elastic free energy in a pure rotation of the center of mass of the volume element at position $\boldsymbol{r}$ with fixed director $\boldsymbol{n}$ [12] and vanishes when all the elastic constants are equal. At steady state, and in most dynamical cases, the inertial terms of the AM balance can be set to zero, which leads to the conservation law of the total angular momentum in the form $\mathrm{div}(\hat{L}+\hat{S})=0$. The SAM and the OAM, however, are not separately conserved, unless $\boldsymbol{w}=0$. The single elastic constant approximation, although widely used in the literature, destroys the spin-orbit coupling in the material and cannot be accepted in any realistic model, and thus will not be retained in our model.

II. THE MODEL

We consider a homeotropically aligned NLC film of thickness L illuminated at normal incidence by a circularly polarized monochromatic optical beam of wavelength λ [Fig. 1(a)]. The boundary conditions imposed to the molecular director $\boldsymbol{n}=(\sin\Theta\cos\Phi,\sin\Theta\sin\Phi,\cos\Theta)$ are $\Theta(x,y,z=0,t)=\Theta(x,y,z=L,t)=0$ and $\partial_z\Phi(x,y,z=0,t)=\partial_z\Phi(x,y,z=L,t)=0$, where the polar z axis is directed along the normal to the sample walls [Fig. 1(b)]. We may then write the fields $\Theta(\boldsymbol{r},t)$ and $\Phi(\boldsymbol{r},t)$ as

$$\Theta(\boldsymbol{r},t)=\sum_{m=1}^{\infty}\Theta_m(x,y,t)\sin\left(\frac{m\pi z}{L}\right),$$

$$\Phi(\boldsymbol{r},t)=\phi_0(x,y,t)+\sum_{m=1}^{\infty}\phi_m(x,y,t)U_m\left[\cos\left(\frac{\pi z}{L}\right)\right], \quad (1)$$

where $U_m[\cdot]$ are the Chebyshev polynomials of the second kind and the mode amplitudes Θ_m, ϕ_m, and ϕ_0 *a priori* depend on the transverse coordinates (x,y) and time t. We assume the transverse intensity profile of the beam at the sample position to have a Gaussian shape with different waists w_x and w_y along the x and y directions, namely, $I(x,y)=I_0\exp[-2(x^2/w_x^2+y^2/w_y^2)]$, which corresponds in practice to a TEM_{00} laser beam that has passed through a cylindrical lens, where $I_0=2P/(\pi w_x w_y)$ and P is the power of the incident light beam. Without loss of generality, we may take $w_x\geqslant w_y$ [Fig. 1(c)]. Assuming the sample thickness much shorter than the Rayleigh range of the incoming beam focused at the sample position, $I(x,y)$ can be taken unchanged throughout the whole film. In practice, this corresponds to $w_{x,y}\gg 2$ μm, which is the case in the reported practical situations [6,7,11].

When the incident power P is above the OFT threshold value, P_{th}, the initial homeotropic alignment is broken and Θ becomes nonzero in the illuminated region, which we further consider to have a Gaussian profile in the transverse plane. More precisely, we assume all the mode amplitudes Θ_m to be proportional to a common transverse Gaussian profile $g(x,y,t)$, $\Theta_m=g(x,y,t)\theta_m(t)$, with

$$g(x,y,t)=\exp\{-2[x\cos\gamma(t)+y\sin\gamma(t)]^2/w_1(t)^2 - 2[-x\sin\gamma(t)+y\cos\gamma(t)]^2/w_2(t)^2\}, \quad (2)$$

where $w_{1,2}$ and γ are functions of time only [Fig. 1(d)]. For the sake of simplicity, the rotational mode ϕ_0 and spatial modes amplitudes ϕ_m are further considered to be functions of time only. Since we checked in a previous work [10] that, to recover the proper sequence of bifurcations in the plane-wave limit ($w_{x,y}/L\to\infty$), only three spatial modes in Θ and Φ are enough, we can safely truncate the sums in Eqs. (1) to $m_{\max}=3$. From Eq. (2) we see that the inhomogeneously reoriented NLC film in the transverse plane is analog to a cylindrical lens whose axis makes an angle γ with respect to the major axis of the beam intensity profile [that is the x axis, see Figs. 1(c) and 1(d)], from which OAM transfer is expected when $\gamma\neq(0,\pi/2)$ [13]. Concerning SAM transfer, it is ensured by a nonzero reorientation, $\Theta\neq 0$.

The derivation of the set ODEs that describes the dynamics of the system starts from the knowledge of the elastic free energy density F_{el}, the optical free energy density F_{opt} and the dissipation function density R of the NLC whose expressions can be found in many textbooks about liquid crystals (e.g. [10]). Although a full hydrodynamic description is possible, the velocity is neglected in our study since the flow caused by the director reorientation was shown to lead to quantitative rather than to qualitative changes in the plane-wave limit [14]. First, we note that, under present descriptions of the system, we get ten time-dependent parameters $\boldsymbol{p}=(\phi_0,\phi_1,\phi_2,\phi_3,\gamma,\theta_1,\theta_2,\theta_3,w_1,w_2)$. Then, the total elastic free energy $\mathcal{F}_{\mathrm{el}}(p_i)$, the total optical free energy $\mathcal{F}_{\mathrm{opt}}(p_i)$ and the total dissipation function $\mathcal{R}(p_i,\dot{p}_i)$ are, respectively, calculated by integrating F_{el}, F_{opt}, and R over the sample

volume using the above material reorientation and light beam intensity profiles, where $\dot{p}_i \equiv \partial p_i / \partial t$. Explicit analytical expressions of $\mathcal{F}_{\rm el}$, $\mathcal{F}_{\rm opt}$, and $\mathcal{R}$ are obtained by assuming small mode amplitudes θ_m and ϕ_m and truncating the corresponding series expansion up to the fourth order included. In contrast, note that no approximation is made on w_1, w_2, γ, and ϕ_0 that may be large at will. Finally, the ten-dimensional set of ODEs,

$$\dot{\boldsymbol{p}} = \boldsymbol{F}(\boldsymbol{p}), \tag{3}$$

is obtained from $\partial \mathcal{R} / \partial \dot{p}_i = -\partial(\mathcal{F}_{\rm el} + \mathcal{F}_{\rm opt}) / \partial p_i$ with $(i = 1, \ldots, 10)$. The analytical expressions of the system given by Eq. (3) is cumbersome and will be given in a forthcoming longer paper.

The numerical integration of the above ODE system accounts for exact calculation of the light propagation problem, noting that the polarization state of light inside the material is nonuniform and depends on the NLC reorientation. Our main assumption is to consider a z-dependent polarization field and calculate at $x=y=0$ where the intensity is maximum. More precisely, the four z-dependent Stokes parameters $S_0 = |E_x|^2 + |E_y|^2$, $S_1 = |E_x|^2 - |E_y|^2$, $S_2 = 2\,\mathrm{Re}(E_x^* E_y)$, and $S_3 = 2\,\mathrm{Im}(E_x^* E_y)$ are necessary to evaluate the electric field in the right-hand side of Eq. (3) for each time step t_j of the integration process. Three independent equations are obtained from the evolution of the reduced Stokes vector $\boldsymbol{s} = \boldsymbol{S}/S_0$ under the geometrical optics approximation,

$$\frac{\partial \boldsymbol{s}}{\partial z} = \frac{2\pi}{\lambda}[n_e(0,0,z,t_j) - n_o]\boldsymbol{\Omega} \times \boldsymbol{s}, \tag{4}$$

with $\boldsymbol{\Omega} = [\cos(2\Phi), \sin(2\Phi), 0]$ and $n_{e,o}$ the extraordinary and ordinary refractive indices [15]. The fourth equation is obtained from the pair of coupled equations that describes the propagation of o/e-waves [10], which gives

$$\frac{\partial S_0}{\partial z} = -S_0 \frac{1}{2n_e}\frac{\partial n_e}{\partial z}[1 + s_1 \cos(2\Phi) + s_2 \sin(2\Phi)]. \tag{5}$$

In numerical calculations, we used as parameters wavelength $\lambda = 532$ nm, film thickness $L = 50$ μm, dielectric permittivities perpendicularly and along the director $\epsilon_\perp = 2.335$ and $\epsilon_\parallel = 3.108$, Frank elastic constants $K_1 = 11.1 \times 10^{-12}$ N, $K_2 = 5.8 \times 10^{-12}$ N, and $K_3 = 16.0 \times 10^{-12}$ N, the material parameters being the ones of the E7 liquid crystal mixture.

III. RESULTS

We introduce the beam shape anisotropy $\mu = w_x / w_y$ $(\mu \geqslant 1)$ and the finite beam size parameter $\delta = 2w_y / L$, which define the light-matter interaction geometry. Depending on (δ, μ), a rich reorientation dynamical behavior is found by taking the beam intensity as the control parameter. For convenience we define the normalized intensity $\rho = I_0 / I_{\rm OFT}$, where $I_{\rm OFT} = 2\pi^2 c \epsilon_\parallel K_3 / (L^2(\epsilon_\parallel - \epsilon_\perp)\sqrt{\epsilon_\perp})$, with c the light speed, is the OFT threshold intensity under circularly polarized excitation, and the normalized time $\tau = t / \tau_{\rm NLC}$, where $\tau_{\rm NLC} = \gamma_1 L^2 / (\pi^2 K_3)$ is a characteristic reorientation time, γ_1 being the rotational viscosity [12]. In addition, we will use the total phase delay

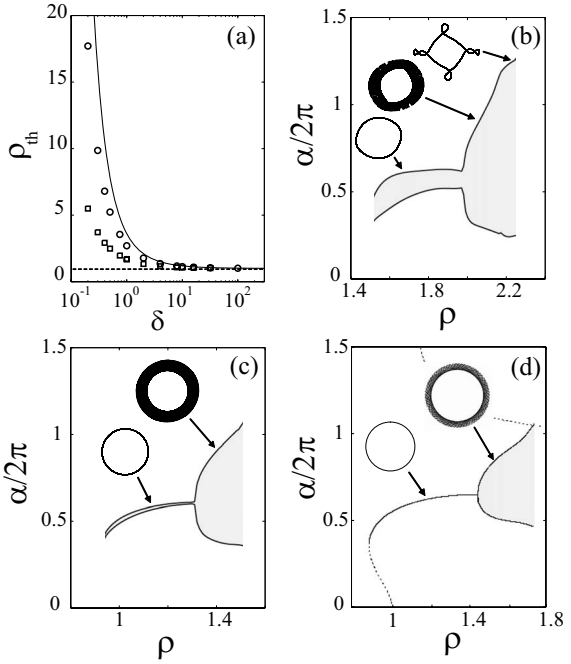

FIG. 2. (a) Reorientation threshold $\rho_{\rm th}$ as a function of δ for $\mu = 1$ (circles) and $\mu = 10$ (squares). The solid line corresponds to the analytical prediction in the single elastic constant approximation and dashed line is the $\rho_{\rm th} = 1$ reference. (b-d) Reorientation diagram $\alpha/2\pi$ vs ρ for $\mu = 10$ with $\delta = 1$ (b), $\delta = 10$ (c), and $\delta \to \infty$ (d). The solid line corresponds to maximum and minimum values reached during dynamics. Insets show typical director trajectories in the (n_x, n_y) plane.

$$\alpha(t) = \frac{2\pi}{\lambda}\int_0^L [n_e(0,0,z,t) - n_o]dz, \tag{6}$$

between the extraordinary and ordinary waves along the beam axis ($n_{e,o}$ are the refractive indices), as a measure of the overall reorientation amplitude [16]. A complete analysis of the director dynamics is postponed in a forthcoming work and hereafter we illustrate the model capabilities in the most complex case where both SAM and OAM are exchanged between the light field and the NLC $(\mu \neq 1)$, and we will restrict ourselves to the situation $\mu = 10$ that corresponds to previously reported experimental works [6,7].

We first check the plane-wave limit behavior (i.e., $\delta \to \infty$) for the reorientation threshold $\rho_{\rm th}$ as shown in Fig. 2(a). For $\mu = 10$ (square symbols) the plane-wave limit $\lim_{\delta \to \infty}(\rho_{\rm th}) = 1$ is obtained. The comparison with the case $\mu = 1$ (circle symbols) and the analytical formula $\rho_{\rm th} = [1 + 2^{3/2}/(\pi\delta)]^2$ for the single-constant approximation (solid line) emphasizes, respectively, the contribution of the beam shape and the elastic anisotropy in the finite beam size effects on the optical Fréedericksz threshold.

Next, the dependence of the dynamical scenario for director reorientation on finite size effects is summarized in Figs. 2(b)–2(d) where the evolution of the diagrams $\alpha/2\pi$ vs ρ as a function of δ is shown. Note that, in these figures, only intermediate reorientation amplitude regimes (i.e, $\alpha/2\pi \sim 1$) are shown. However, small reorientation amplitude regimes

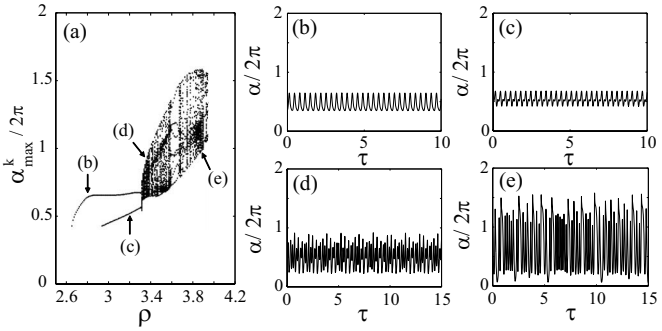

FIG. 3. Bifurcation diagrams for $\delta=0.4$, $\mu=10$ (a) snapshots of $\alpha(\tau)/2\pi$ for $\rho=2.80$ (b), 3.20 (c), 3.35 (d), 3.92 (e), which illustrate periodic (b,c), quasiperiodic (d), and aperiodic (3) dynamics.

(i.e, $\alpha/2\pi \sim 0.01$) are also found in agreement with observations [9], whose thorough discussion is postponed together with the details of the model's equations. As expected from a self-consistent model, the bifurcation diagram uniformly converges toward the plane-wave situation as shown from the sequence of Figs. 2(b)–2(d). In addition we found that new regimes appear when δ decreases, as illustrated by the inset director trajectories in the (n_x,n_y) plane.

Actually, the dynamics is as much enriched as the finite beam size effects are pronounced in agreement with the experimental studies [17]. In particular, a complex sequence of rotational director dynamics is found for sufficiently small δ. Figure 3 is a representative example of such a trend, where $\delta=0.4$. In Fig. 3(a) the local maxima of $\alpha(\tau)$, $\alpha_{\max}^{(k)}$, are plotted as a function of ρ. The four snapshots in panels (b), (c), (d), and (e) illustrate various dynamical regimes, namely, periodic, quasiperiodic, or aperiodic, for some values of ρ as indicated by arrows in panel (a).

Chaotic rotations are also found, which are charaterized by a long-term uniform azimuthal motion, $\phi_0(\tau) \propto \Omega\tau$, together with a chaotic dynamics of the reorientation amplitude, as observed in the experiments [6]. This is illustrated in Fig. 4, where the director trajectory in the (n_x,n_y) plane exhibits the typical features of a chaotic attractor [Fig. 4(a)] with a "noisy" Fourier spectra [Fig. 4(b)] and a long-term uniform motion of the rotational mode [Fig. 4(c)].

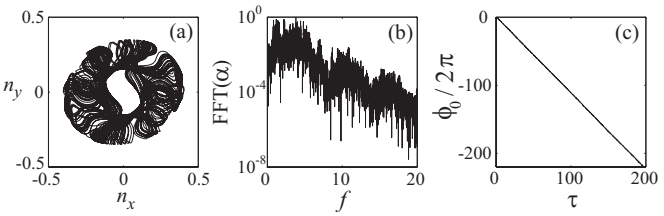

FIG. 4. Complex rotation dynamics for $\delta=0.4$, $\mu=10$, and $\rho=3.91$. (a) Director trajectory in the (n_x,n_y) plane. (b) Fourier spectrum of α where f is the normalized frequency. (c) $\phi_0(\tau)/2\pi$ illustrating of the long-term uniform rotational motion.

IV. CONCLUSION

We derived a full three-dimensional model able to describe the orientational dynamics of a nematic liquid crystal film under a laser beam of arbitrary shape and polarization. Our approach accounts for light spin and orbital angular momentum transfer processes and the internal torque due to the elastic anisotropy of the liquid crystal. We conclude from our study that higher order spatial reorientation modes have necessarily to be taken into account together with the exact calculation of the nonadiabatic propagation of light in order to obtain a self-consistent model. On the one hand, a satisfying behavior for the optical Fréedericksz threshold and the optically induced dynamics beyond threshold as a function of finite beam size effects is obtained. On the other hand, complex dynamical regimes are described when the beam cross section is sufficiently small as compared to the liquid crystal film thickness. In particular, collective molecular chaotic rotations have been described in presence of both spin and orbital angular momentum exchanges between light and matter in agreement with previous experimental findings.

[1] T. Yalçinkaya and Y.-C. Lai, Phys. Rev. Lett. **79**, 3885 (1997).
[2] E. Rosa, E. Ott, and M. H. Hess, Phys. Rev. Lett. **80**, 1642 (1998).
[3] B. Blasius, A. Huppert, and L. Stone, Nature (London) **399**, 354 (1999).
[4] E. N. Lorenz, J. Atmos. Sci. **20**, 130 (1963).
[5] O. E. Rössler, Phys. Lett. **57A**, 397 (1976).
[6] A. Vella, A. Setaro, B. Piccirillo, and E. Santamato, Phys. Rev. E **67**, 051704 (2003).
[7] E. Brasselet and L. J. Dubé, Phys. Rev. E **73**, 021704 (2006).
[8] Y. Kuramoto, in *International Symposium on Mathematical Problems in Theoretical Physics*, edited by H. Araki, Lecture Notes in Physics No. 30 (Springer, New York, 1975), p. 420.
[9] B. Piccirillo, A. Vella, A. Setaro, and E. Santamato, Phys. Rev. E **73**, 062701 (2006).
[10] E. Brasselet, T. V. Galtsian, L. J. Dubé, D. O. Krimer, and L. Kramer, J. Opt. Soc. Am. B **22**, 1671 (2005).
[11] B. Piccirillo and E. Santamato, Phys. Rev. E **69**, 056613 (2004).
[12] P. G. de Gennes, *The Physics of Liquid Crystals* (Oxford University Press, Oxford, 1974).
[13] B. Piccirillo, A. Vella, and E. Santamato, Phys. Rev. E **69**, 021702 (2004).
[14] D. O. Krimer, G. Demeter, and L. Kramer, Phys. Rev. E **71**, 051711 (2005).
[15] E. Santamato, G. Abbate, and P. Maddalena, Phys. Rev. A **38**, 4323 (1988).
[16] N. V. Tabiryan, A. V. Sukhov, and B. Y. Zel'dovich, Mol. Cryst. Liq. Cryst. **136**, 1 (1986).
[17] E. Brasselet, B. Doyon, T. V. Galtsian, and L. J. Dubé, Phys. Rev. E **69**, 021701 (2004).